Copropagating pump and probe experiments on Si-nc in SiO$_2$ rib waveguides doped with Er: The optical role of non-emitting ions

D. Navarro-Urrios,[1,a)] F. Ferrarese Lupi,[1] N. Prtljaga,[2] A. Pitanti,[2,3] O. Jambois,[1] J. M. Ramírez,[1] Y. Berencén,[1] N. Daldosso,[2,4] B. Garrido,[1] and L. Pavesi[2]

[1]*MIND-IN2UB, Dept. Electrònica, Universitat de Barcelona, C/Martí i Franquès 1, 08028 Barcelona, Spain*
[2]*Laboratorio di Nanoscienze, Dipartimento di Fisica, Università di Trento, Via Sommarive 14, I-38100 Povo (Trento), Italy*
[3]*NEST, Scuola Normale Superiore, Istituto di Nanoscienze-CNR, Piazza San Silvestro 12, 56127 Pisa, Italy*
[4]*Dipartimento di Informatica, Università di Verona, Strada Le Grazie 15, 37134 Verona, Italy*

We present a study that demonstrates the limits for achieving net optical gain in an optimized waveguide where Si nanoclusters in SiO$_2$ codoped with Er^{3+} are the active material. By cross correlating absorption losses measurements with copropagant pump ($\lambda_{pump} = 1.48\,\mu$m) and probe ($\lambda_{probe} = 1.54\,\mu$m) experiments we reveal that the role of more than 80% of the total Er^{3+} population present on the material (intended for optical amplification purposes) is to absorb the propagating light, since it is unfeasible to invert it. © *2011 American Institute of Physics.* [doi:10.1063/1.3665950]

Within the last decade, lots of efforts have been dedicated towards the realization of the "holy grail" of silicon photonics, i.e., a monolithic silicon optical amplifier or laser. As an active medium for achieving this goal, Si nanoclusters (Si-nc) in dielectric matrices coupled to Er^{3+} ions have been one of the most promising alternatives.[1] Initial reports of internal optical gain on strip waveguides contributed to raise further the expectations.[2–4] Most of the works present in the literature are focused on the understanding of the physical characteristics of the Si-nc to Er^{3+} transfer and the optimization of the coupled content, where a maximum of just few tens percents was achieved.[5–9] But even though those are certainly key issues towards the optimization of the material, yet a more disturbing feature is the existence of a sizeable Er^{3+} population (up to more than 80% of the total content) that is not emitting light efficiently, even under direct pumping.[10–12] The few reports present in the literature focused on this Er^{3+} content did not study the optical role that those dark ions may play from the point of view of an optical amplification application, i.e., if they are just transparent or they absorb light. The present letter addresses this issue in a conclusive way by comparing the absorption with maximum amplification values measured on a rib loaded waveguide, whose active layer is composed of an optimized material.

The sample under analysis has been produced by using standard deposition processes. Initially, 5 μm of SiO$_2$ have been deposited above a crystalline Si substrate, becoming the optical bottom cladding of the waveguides. The active layer has afterwards been fabricated by means of a RF reactive magnetron co-sputtering method of 2-in. confocal pure SiO$_2$ and Er$_2$O$_3$ targets under Argon-Hydrogen gas mixture.[13] As a result, 1.2 μm of substoichiometric silicon-rich silicon oxide (SRSO) doped with Er^{3+} ions have been deposited. A further top cladding layer of 1 μm of SiO$_2$ has been finally grown. This was followed by an annealing treatment under a pure nitrogen flow to promote phase separation between silicon and its oxide in the active layer. The various deposition parameters (H$_2$ partial pressure, substrate temperature during active layer deposition and annealing temperature) have been varied for optimising two main figures of merit: the PL intensity under non-resonant pumping ($\lambda = 476$ nm) and the lifetime of the ^{4}I$_{13/2} \rightarrow ^4$I$_{15/2}$ Er^{3+} transition.[13,14] This manuscript deals with the best layer obtained following this optimisation. Its composition was measured by x-ray photoelectron spectroscopy and secondary ions mass spectroscopy, presenting a Si excess of about 5% and an Er^{3+} content of $3.4 \pm 0.2 \times 10^{20}$ cm^{-3}. The layer has been annealed at 910 °C during 60 min, so it likely contains Si in an amorphous nanocluster form. The active material has the same nominal composition of sample A from Refs. [6] and [15] and sample B from Ref. [12].

In order to produce monomodal rib-loaded waveguides with high confinement factor, a dry etching of the top SiO$_2$ cladding has been performed down to 200 nm over the active layer. We will report on 5 μm wide waveguides (see Fig. [2] for a waveguide profile).

The optical losses of the waveguides have been determined by means of the cut-back technique along the spectral range provided by a tunable laser (from 1460 to 1580 nm). A tapered fiber was used to butt-couple the input light, leading to coupling losses of about 4 dB.

The evaluation of the cross section at 1480 nm from time resolved μ-PL measurements has been performed following the procedure described in a previous work.[12]

Pump and probe experiments were carried out to evaluate the signal enhancement (SE) of a probe signal coupled to the waveguides, when a pump signal is also present.[4] We have used as a probe signal a tunable laser and as a pump signal a high power diode laser emitting at 1.48 μm (far away from the absorption spectrum of Si-nc). Both lasers have been combined in a wavelength-division-multiplexer (WDM) fiber, connected to a tapered fiber and finally butt-coupled into the active waveguide. In order to filter out the contribution of the amplified spontaneous emission (ASE)

a)Electronic mail: dnavarro@el.ub.es. Present address: Catalan Institute of Nanotechnology (CIN2-CSIC), Campus UAB, Edifici CM3, 08193 Bellaterra, Spain.

99, 231114-1

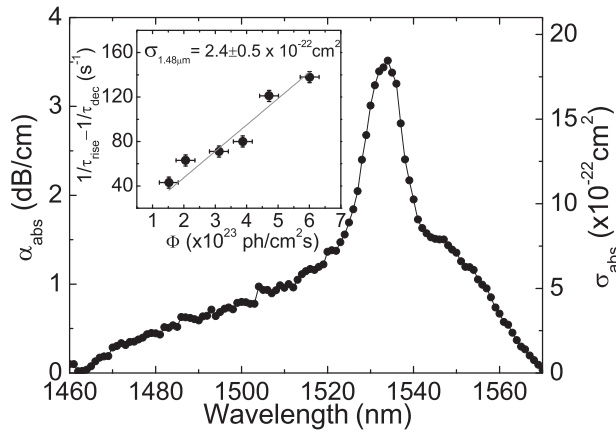© 2011 American Institute of Physics

FIG. 1. Spectral dependence of the absorption losses (left axis) and of the absorption cross section (right axis). Inset: difference of the inverses of the rise and decay lifetimes as a function of Φ. The gray curve corresponds to the linear fit used to extract σ_{abs}.

signal related to the pump we have modulated the probe signal and used a lock-in at the detection stage.

As an initial step we have quantified the spectral losses of the waveguide. The raw insertion loss spectrum showed the Er^{3+} related absorption peak superimposed to a background that decreases by increasing the wavelength. Those background losses values were about (3.0 ± 0.5) dB/cm at 1535 nm and (4.0 ± 0.5) dB/cm at 1480 nm and are associated to passive scattering losses from the Si nanostructures present in the matrix and the matrix itself.[16] On Fig. 1 we show the result of subtracting those passive losses from the propagation losses, the remaining contribution being that associated to the direct absorption losses (α_{abs}) of Er^{3+}. It is worth to mention that α_{abs} is related to the total Er^{3+} absorbing content (N_{abs}) by the following relation:

$$\alpha_{abs}(\text{dB/cm}) = 4.34 \sigma_{abs} N_{abs} \Gamma, \tag{1}$$

where Γ is the confinement factor of the waveguides ($\Gamma = 0.8$ as extracted from beam propagation method (BPM) simulations) and σ_{abs} is the absorption cross section at the tested wavelength. It is important to note that the maximum of absorption losses is about (3.5 ± 0.2) dB/cm at 1534 nm. Therefore, if full population inversion is achieved, the inter-
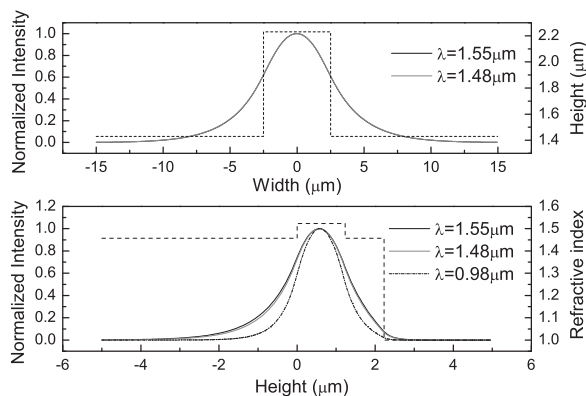

FIG. 2. (a) Horizontal shape of the supported modes at 1.54 μm (black) and 1.48 μm (gray). The horizontal profile of the waveguide is also shown (dashed line). (b) Vertical shape of the supported modes at 1.54 μm (solid black), at 1.48 μm (gray) and at 0.98 μm (dash dotted black). The vertical profile of the refractive index of the waveguide is also shown (dashed line).

nal gain values would compensate for the passive losses and net optical gain of about 0.5 dB/cm would be possible.

It is possible to extract the spectral shape of σ_{abs} by estimating it at a certain wavelength and then using the spectral shape of the absorption losses. We have done this procedure at $\lambda = 1.48 \mu$m with high photon flux (Φ) time resolved PL measurements.[12] The difference of the inverses of the lifetimes as a function of Φ is a linear curve whose slope is proportional to σ_{abs} at the pumping wavelength. In the inset of Fig. 1 these data are presented, providing a value of σ_{abs} $(1.48 \mu\text{m}) = (2.4 \pm 0.5) \times 10^{-22} \text{cm}^2$. If we apply the McCumber relationship for extracting the emission cross section ($\sigma_{em}(\upsilon) = \sigma_{abs}(\upsilon) e^{\frac{\varepsilon - h\upsilon}{kT}}$, where ε is the average energy of the transition, k the Boltzmann constant, and T the temperature), it is possible to calculate that $\sigma_{em}(\lambda = 1.48 \mu\text{m})$ is about 4 times lower than $\sigma_{abs}(\lambda = 1.48 \mu\text{m})$.

Moreover, from σ_{abs} and Eq. (1) the concentration of absorbing Er^{3+} can be calculated to be $N_{abs} = (4.9 \pm 1.0) \times 10^{20} \text{cm}^{-3}$. N_{abs} is slightly higher than the total content measured by SIMS, but compatible with this value. Even though there is a sizeable error bar derived from the entire experimental procedure, we can state that most of Er^{3+} absorbs.

To determine the concentration of emitting Er^{3+} (N_{em}), we have performed pump and probe measurements. Since excitation is performed at 1.48 μm, we can assume an effective two level system to describe the population of the $^4I_{13/2}$ level (N_2) and of the $^4I_{15/2}$ level (N_1), being $N_1 + N_2 = N_{em}$.

In Fig. 2, we show the profile of the TE mode in the horizontal (top panel) and vertical (bottom panel) directions for $\lambda = 1.48 \mu$m (pump) and $\lambda = 1.54 \mu$m (probe) wavelengths as extracted from beam propagation method (BPM) simulations. The overlap between the pump and the probe optical modes is higher than 98%.

The ratio between the probe signal with the pump on ($I_{pump\&probe}$) and the probe signal with the pump off (I_{probe}) is defined as the SE measured at the output of the waveguide. We will assume the emission and absorption cross sections (σ_{em} and σ_{abs} respectively) to be equal, which are reasonable around the maximum of the emission-absorption spectrum and take into account the stimulated emission contribution at the pump wavelength. Under those circumstances, SE and the internal gain (g_{int}) are

$$SE = \frac{e^{(N_2 \sigma_{em} - N_1 \sigma_{abs})\Gamma L}}{e^{-N_{Em}\sigma_{abs}\Gamma L}} \approx e^{2\sigma_{abs}\frac{\sigma_{exc}N_{Em}\Phi}{\frac{1}{\tau_d}+1.25\sigma_{exc}\Phi}\Gamma L} = e^{2g_{int}L}, \tag{2}$$

$$g_{int}(\text{dB/cm}) = 4.34 \sigma_{abs} \frac{\Phi \sigma_{exc} N_{em}}{\frac{1}{\tau_d} + 1.25 \Phi \sigma_{exc}} \Gamma = \frac{G_{int}}{L}, \tag{3}$$

where G_{int} is the total internal gain, τ_d is the decay lifetime of the $^4I_{13/2} \rightarrow {}^4I_{15/2}$ transition, $\sigma_{exc} = \sigma_{abs}(1.48 \mu\text{m})$, and L is the length of the waveguide. Note that Φ is reported at the input waveguide facet and decays along the waveguide with approximately 4 dB/cm loss. For low Φ, $\tau_d^{-1} \gg \Phi\sigma_{exc}$ and $g_{int} = \tau_d \sigma_{abs} N_{em} \sigma_{exc} \Gamma \Phi$, linear in Φ.

In Fig. 3(a), the spectral dependences of SE for low and high Φ are reported for a 6 mm long waveguide (black squares and red dots respectively). By comparing these two measurements it is clear how SE increases with Φ. For a 14 mm long waveguide (green triangles in Fig. 3(a)) it is possible to enhance further SE in an almost exponential way, revealing
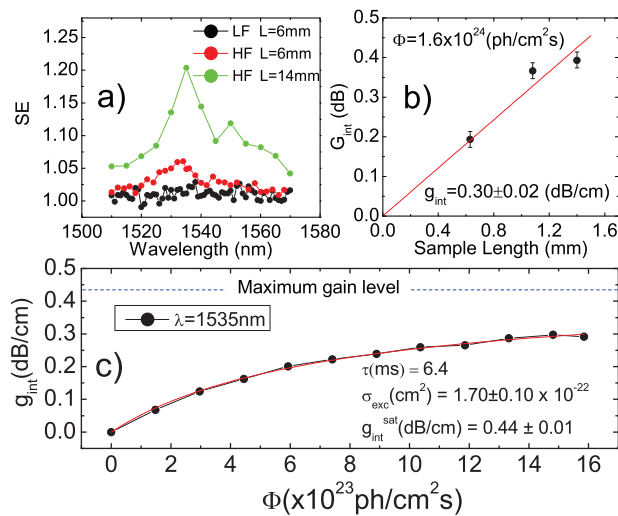
FIG. 3. (Color online) (a) SE of a 6 mm long waveguide at low and high Φ (black squares and red dots, respectively) and of 14 mm long waveguide at high Φ (green triangles). (b) G_{int} for different waveguide lengths at high Φ. A linear fit to the data is also shown. (c) g_{int} as a function of Φ for a waveguide length of 6 mm. A fit using Eq. (3) is also shown.

very clearly the Er^{3+} signature. Fig. 3(b) shows G_{int} as a function of the waveguide length for the high Φ. From the linear fit of the data, a g_{int} of about 0.3 dB/cm can be extracted. The deviation from the linear behavior is due to a pump depletion. Finally, in Fig. 3(c) we show g_{int} at $\lambda = 1535$ nm as a function of Φ for the shortest waveguide. The experimental data present a sublinear behavior, which is a clear indication that saturation is close to be achieved although not yet reached due to pump power limitations. We report a maximum value of $g_{int} = 0.3$ dB/cm at $\Phi = 1.6 \times 10^{24}$ (ph/cm^2 s), with an error of less than 5%. The experimental points are fit by Eq. (3), where $\tau_d = 6.4$ ms as extracted from the pure exponential behavior of the $^4I_{13/2} \rightarrow {}^4I_{15/2}$ PL decay. The fit yields two parameters: σ_{exc} and g_{int} at saturation, g_{int}^{sat}. The best fit is shown in Fig. 3(c) as a line. The first best fit parameter results $\sigma_{exc} = (1.7 \pm 0.1) \times 10^{-22}$ cm^{-2}, which is similar to the one derived by the analysis of Fig. 1. The second best fit parameter is $g_{int}^{sat} = (0.44 \pm 0.01)$ dB/cm, which could be 0.55 dB/cm in the absence of pump induced stimulated emission. The latter value is just (16 ± 2)% of the absorption at the same wavelength (Fig. 1). From this result it is straightforward to conclude that most of the Er^{3+} within the matrix is able to absorb but cannot emit light efficiently. Even more, within the approximation of equal absorption and emission cross sections, we could conclude that 84% of the Er^{3+} population cannot be inverted. In a previous work, we have reported that the maximum Er^{3+} content able to emit light efficiently under direct optical pumping was $N_{em} = 0.64 \times 10^{20}$ cm^{-3}.[12] This value is 19% of the total Er^{3+} content present in the sample, which is compatible with the 16% reported here.

Moreover, the emitting Er^{3+} population does not suffer from strong cooperative up-conversion mechanisms.[15] Therefore, based on all the previous observations, we postulate the existence of two Er^{3+} ions: (i) one able to recombine radiatively with roughly the same probability and (ii) another surrounded by quenching centers where the radiative recombination probability is extremely small. Although it is not the intention of the paper to provide a thorough insight of the microscopic physical properties of the non-emitting Er^{3+} ions, we are of the opinion that they may be placed within the Si-nc or that they clusterize and suffer from quenching effects. Indeed, it has already been reported in bulk glasses that the concentration of Er^{3+} is not homogeneous and clusters of ions can locally form whereas elsewhere they are isolated.[17,18] In all cases, the fact that more than 80% of the Er^{3+} acts as absorber is the first indispensible step of knowledge towards a clear understanding of those ions, which may allow optimizing the emitting and coupled content beyond the threshold of transparency.

In conclusion, we have reported on the absorption and amplification properties of an optimized waveguide with Si-nc coupled to Er^{3+} in a SiO_2 matrix as an active layer. By comparing the absorption losses and the maximum achievable internal gain we have determined that only 16% of the Er^{3+} ions can be inverted, even under resonant copropagant pumping, the rest 84% contributing only to absorption. The extracted internal gain values are conclusive since: (i) the spatial distribution of the waveguide modes for the pump and probe wavelengths is practically equivalent, (ii) the internal gain values are almost driven to saturation, (iii) the pump light suffers low losses, so it can pump effectively the whole length of the waveguide. On the basis of these results we conclude that net optical gain under optical pumping is still far to be accomplished.

[1] D. Liang and J. E. Bowers, Nat. Photon. **4**, 511 (2010).
[2] J. H. Shin, H. S. Han, and S. Y. Seo, *Towards the First Silicon Laser*, edited by L. Pavesi, S. V. Gaponenko, and L. Dal Negro (Kluwer, Dordrecht, 2003), NATO Science Series II, Vol. 93, p. 401.
[3] J. Lee, J. H. Shin, and N. Park, J. Lightwave Technol. **23**, 19 (2005).
[4] N. Daldosso, D. Navarro-Urrios, M. Melchiorri, L. Pavesi, F. Gourbilleau, M. Carrada, R. Rizk, C. Garcia, P. Pellegrino, B. Garrido, and L. Cognolato, Appl. Phys. Lett. **86**, 261103 (2005).
[5] B. Garrido, C. García, S.-Y. Seo, P. Pellegrino, D. Navarro-Urrios, N. Daldosso, L. Pavesi, F. Gourbilleau, and R. Rizk, Phys. Rev. B **76**, 245308 (2007).
[6] A. Pitanti, D. Navarro-Urrios, N. Prtljaga, N. Daldosso, F. Gourbilleau, R. Rizk, B. Garrido, and L. Pavesi, J. Appl. Phys. **108**, 053518 (2010).
[7] M. Wojdak, M. Klik, M. Forcales, O. B. Gusev, T. Gregorkiewicz, D. Pacifici, G. Franzò, F. Priolo, and F. Iacona, Phys. Rev. B **69**, 233315 (2004).
[8] P. G. Kik and A. Polman, J. Appl. Phys. **88**, 1992 (2000).
[9] I. Izeddin, A. S. Moskalenko, I. N. Yassievich, M. Fujii, and T. Gregorkiewicz, Phys. Rev. Lett. **97**, 207401 (2006).
[10] S. Minissale, T. Gregorkiewicz, M. Forcales, and R. G. Elliman, Appl. Phys. Lett. **89**, 171908 (2006).
[11] P. Pellegrino, B. Garrido, J. Arbiol, C. Garcia, Y. Lebour, and J. R. Morante, Appl. Phys. Lett. **88**, 121915 (2006).
[12] D. Navarro-Urrios, Y. Lebour, O. Jambois, B. Garrido, A. Pitanti, N. Daldosso, L. Pavesi, J. Cardin, K. Hijazi, L. Khomenkova, F. Gourbilleau, and R. Rizk, J. Appl. Phys. **106**, 093107 (2009).
[13] F. Gourbilleau, C. Dufour, M. Levalois, J. Vicens, R. Rizk, C. Sada, F. Enrichi, and G. Battaglin, J. Appl. Phys. **94**, 3869 (2003).
[14] F. Gourbilleau, M. Levalois, C. Dufour, J. Vicens, and R. Rizk, J. Appl. Phys. **95**, 3717 (2004).
[15] D. Navarro-Urrios, A. Pitanti, N. Daldosso, F. Gourbilleau, L. Khomenkova, R. Rizk, and L. Pavesi, Physica E **41**, 1029 (2009).
[16] N. Daldosso, D. Navarro-Urrios, M. Melchiorri, C. García, P. Pellegrino, B. Garrido, C. Sada, G. Battaglin, F. Gourbilleau, R. Rizk, and L. Pavesi, IEEE J. Sel. Top. Quantum Electron. **12**, 1607 (2006).
[17] B. J. Ainslie, S. P. Craig-Ryan, S. T. Davey, J. R. Armitage, C. G. Atkins, J. F. Massicott, and R. Wyatt, IEE Proc.-J: Optoelectron. **137**, 205 (1990).
[18] B. J. Ainslie, J. Lightwave Technol. **9**, 220 (1991).